THE GLASS ANNEALING PROCESS IN LABORATORY CONDITIONS AND ITS CONTROL

STANISLAV KASA, ANTONÍN LISÝ, ROMAN RANDÁK*

Department of Glass Technology, Institute of Chemical Technology, Technická 5, 166 28 Prague 6
** Rapotín Glassworks, 788 14 Rapotín*

Received 24. 6. 1991

In accordance with the theoretical analysis of glass annealing process a laboratory kiln has been calculated, designed and constructed. This kiln has been completed by control and measuring instruments which allowed the comparison of the temperature regime, with the pre-calculated annealing curve. For the control of annealing process the computer SAPI 1 equipped with a compiled software programme have been used. The control of glass annealing process and its quality has been verified by several samples of sheet glass. A very good correspondence between the calculated and measured values of mechanical stresses in glass has been found.

1. INTRODUCTION

Annealing of glass is a controlled heat treatment process eliminating excessive internal stresses in glass ware and preventing them from forming. For assuring a satisfactory quality of annealed ware, it is necessary to adjust suitably the thermal process in the annealing lehr. Most of existing production and laboratory lehrs and kilns are designed in such a way that they do not allow the annealing rate to be increased owing to a large thermal capacity of the lining, and a considerable temperature inhomogeneity of the inner atmosphere. To be able to implement the calculated annealing curve in practice, one has to employ an annealing kiln or lehr permitting the outer wall to be cooled efficiently, and providing efficient forced convection of the inner atmosphere.

The glass annealing process is one of non-stationary heat transfer. It can be controlled by suitable computer technology, because the existing analog control methods require interventions by operators who, however, are unable to ensure the required course of the temperature schedule in the lehr. The use of computer technology in the control of technological processes always leads to achieving a high degree of automation, and in most cases allows for the control of even such processes that cannot be controlled by classical means, and if so, then with considerable difficulties involved. Such technological processes also include glass annealing. By adjusting the correct annealing schedule in the lehr and allowing it to be automatically controlled, one can not only improve the quality of the ware, but also cut down the time required for annealing, and in this way saving energy and lowering total production costs.

2. THE KINETICS OF FORMATION AND EQUALIZATION OF INTERNAL STRESSES IN GLASS

The relationships for the formation and relaxation of stresses in viscous bodies were derived by Maxwell [1]. Stress σ due to the effect of a deformation force on a viscous body will not remain constant, being subject to relaxation according to the equation

$$\frac{d\sigma}{d\tau} = -\frac{P_m}{\eta}\sigma = -\frac{1}{\tau_m}\sigma \qquad (1)$$

whose integration within the appropriate limits yields the simple exponential relationship

$$\sigma = \sigma_0 \exp\left(-\frac{\tau}{\tau_m}\right). \qquad (2)$$

In their studies of the annealing of optical glass, Adams and Williamson [2] expected to obtain a simple exponential equation corresponding to Maxwell's concept. However, they did not obtain any linear relation, and on the contrary found the rate of stress relaxation at the respective specimen point not to be proportional to the stress existing at the point, being proportional to its square. This finding led to Adams-Williamson's law, which can be written in the form

$$\frac{d\sigma}{dt} = -K_1\sigma^2 \qquad (3)$$

whose integration yields an equation which till recently had been used in the calculation of annealing procedures. Adams-Williamson's relationship cannot be excessively generalized, as its validity is restricted solely to the conditions under which it has been derived. Namely, these are the relatively low stresses arising in the annealing of optical glass. Eventually, other studies were published [3, 4, 5, 6, 7], which dealt with the problems of calculating the rate of stress relaxation.

3. THE RELATIONS BETWEEN ANNEALING RATE, TEMPERATURE GRADIENTS AND STRESS

The annealing process is one controlled by heat transfer. This is why the following three phase can be observed during its course [1]:

a) the phase of a disarranged process, during which the rate of temperature changes depends strongly on the initial random state;

b) the phase of an orderly process, when the effect of initial irregularities has already decreased down and the temperature changes in the entire product can be described by an exponential equation;
c) the phase of a steady state where the temperature distribution is already constant, and on heating up or cooling from both sides, the temperature in the specimen is identical with the ambient one.

From the standpoint of analytical treatment, the phase of the disarranged process is the most difficult one. However, there is the advantage in that the phase has a negligible effect on the resolving of the entire annealing process. On the other hand, the orderly process stage is the most significant one, that is the stage of cooling the ware down from the annealing temperature, and also the stage of the steady state involving the heating up to annealing temperature and that of final cooling down to ambient temperature.

4. THE RELATIONSHIP BETWEEN THE RATE OF COOLING AND STRESS

The maximum admissible cooling rate, that is the rate of cooling ensuring that the residual stress in the ware does not exceed its strength, is the most important quantity for ensuring the correct result of glass ware annealing. there is a number of equations for calculating the admissible rate of cooling, for example that suggested by Murgatroyd:

$$h_1 = \frac{2a\sigma}{\alpha_D N s^2 E} . \tag{4}$$

Duvalier [5] adjusted equation (4) by taking into account the parabolic distribution of temperature and the elasticity theory:

$$h_1 = \frac{2a(1-\mu)\sigma}{\alpha_D E s^2} . \tag{5}$$

Indenbom [8] derived an equation expressing the relationship between the relaxation time and temperature in exponential form,

$$\tau_r = \tau_0 \exp\left(\frac{T_0 - T}{\Theta}\right) . \tag{6}$$

On the basis of equation (6), the following relation holds for permanent stress at the centre of a plate:

$$\sigma = \frac{\alpha_D E}{1-\mu}\left[1 - \exp\left(-\frac{\Theta}{h_1 \tau_0}\right)\right]\frac{h_1 s^2}{6a} . \tag{7}$$

Equation (7) indicates that at

$$\frac{h_1 \tau_0}{\Theta} \ll 1 \tag{8}$$

the permanent stresses are proportional to the cooling rate, thus conforming to Dauvalter's equation. In the opposite case, stress does not depend on the cooling rate and must be determined according to the annealing temperature.

In deriving his relations for stress vs. rate of cooling, Schill [1] used, as a basis, the temperature gradients arising in the glass ware wall. For example, for a plate whose temperature gradient between the surface and an arbitrary layer x of the body is

$$\Delta T_x = \frac{h_1}{2a}(s^2 - x^2) \tag{9}$$

the stress in a plate $\delta = 2s$ in thickness is given by the equation

$$\sigma = -\frac{E\alpha_D h_1}{6a(1-\mu)}(s^2 - 3x^2) . \tag{10}$$

In a similar way, Schill has derived equations for glass ware of various shapes, such as a cylinder, a full sphere, a hollow sphere, a tube heated from inside or outside [1].

5. THE METHODS FOR CALCULATING THE ANNEALING SCHEDULE

The methods for calculating the annealing schedule can be divided into two groups. The first comprises the so-called semiempirical determination of annealing schedules based on the studies by Adams and Williamson on the assumption that the thermal stress arising in the ware wall in the course of cooling down or heating up, is directly proportional to the temperature gradient, or in other words, directly proportional to the cooling or heating rate.

At present, all authors dealing with the annealing of glass use the following well proved procedure, which divides the annealing process into the following four stages:

1. Heating up to the annealing temperature.
2. Dwell at the annealing temperature.
3. Cooling down in the annealing region.
4. Final cooling down to ambient temperature (20 to 50°C), as described in detail in [1, 9].

The second group comprises computing procedures based on mathematical modelling of the annealing process. The calculations concern the courses of temperature yielded by approximate analytical solutions of the heat conduction equation, or on the basis of empirical equations determined specifically for the given types of glass. However, there is also the possibility of an exact computing procedure based on numerical solution of a system of equations for temperature distribution in the ware, and for the formation and relaxation of stresses and the relaxation of structure. The method was developed in the studies by Mazurin [10, 11, 12] and Januskiewicz [13]. In view of the complexity of the calculations involved, the authors have introduced some simplifying assumptions, such as:

a) The temperature field is calculated for the thickness of an infinite plate.
b) The calculation proceeds from the plate surface to its centre where the heat transfer is assumed to be zero.
c) Thermal conductivity by radiation and conduction are joined into a single effective thermal conductivity.
d) The modulus of elasticity, Poisson' coefficient and density are considered as constants.
e) The product is plate-shaped.

In spite of this simplification, the results of the mathematical modelling show a very satisfactory agreement with theory and practice.

6. EXPERIMENTAL

The experimental work was divided into several consequent stages as follows:

a) Determination of the annealing procedure, including calculations of both basic annealing temperatures and calculation of the annealing curve.
b) Design and construction of a laboratory annealing kiln.
c) Measurement of temperatures.
d) Design and installation of a measuring system for controlled power input supply to the kiln, and for measuring the temperature in the kiln.

6.1 Determination of the annealing procedure

All measurements were carried out on plate-shaped specimens of Float glass 10×10×0.5 cm in size. The upper and lower annealing temperatures were determined according to linear developments for the calculation of the given viscosities (10^{13} and $10^{14.5}$dPa.s) from the chemical composition of the Float glass according to Šašek [14]. For the Float glass specimens in question, it holds that t_{13} = 534°C and $t_{14.5}$ = 489°C. For these temperatures, the basic relative temperature points of annealing were established, i.e. the annealing curves supplemented with entry temperature and the required final temperature of the glass specimen:

- annealing temperature (holding temperature) t_{ch} = 534°C
- temperature of the lower limit of the annealing interval t_d = 434°C
- annealing temperature range Δt = 100°C
- entry temperature of glass t_v = 20°C
- required final temperature of glass t_k = 50°C

The annealing curve was calculated using the procedure described in [9] and the following parameters were obtained:

- the time of heating τ_V = 594 s
- the rate of heating h = 52 K min^{-1}
- the time of cooling τ_i = 237 s
- upper cooling rate h_i = −25.3 K min^{-1}
- final cooling down time τ_2 = 303 s
- lower annealing rate h_2 = −75.9 K min^{-1}

The annealing temperature (of 534°C) was chosen so as to relax all stresses in the glass within 240 s. However, a time reserve of 660 s in the time of holding was considered according to [5] in order to guarantee equalization of temperature gradients in the glass specimens being measured, so that the total time of annealing was

τ_{total} = 594 + 900 + 237 + 303 = 2034 s, i.e. 33.4 minutes.

6.2 Design and construction of the annealing kiln

To carry out the experiments, it was necessary to construct a kiln which would meet the requirements for significant changes in temperature according to the calculated annealing curve. Primarily, a rapid and controlled decrease of temperature had to be ensured in the stage of cooling. This was achieved by extensive cooling of the outer muffle wall by a stream of fan-driven air.

In designing the annealing kiln, the shape factors of the specimen being annealed had also to be taken into account in order to achieve an all-surface, bilateral and uniform heat transmission between the kiln atmosphere and the glass surface. For this reason, the kiln was provided with two separate kanthal heating windings, each controlled individually. The windings were coiled on cordierite plates situated horizontally and mutually parallel in the kiln. The plate-shaped specimen to be annealed was placed, also in horizontal position, on small cordierite beams at the centre between the plates. To ensure that the surface temperature of glass is measured correctly, a propeller providing forced convection of the kiln atmosphere was also fitted inside. The specimen surface temperature was measured on both sides, the corundum capillaries with thermocouples being also horizontally situated so as not to pass through any temperature maximum zone. A schematic diagram of the laboratory annealing kiln is shown in Fig. 1.

From the standpoint of correct operation of the annealing kiln, it was necessary to calculate the maximum heat losses and the total kiln input in order to ensure the desired time dependence of the kiln temperatures according to the annealing curve, and to make up all heat losses through the kiln surface and by the cooling air. The total heating kiln input can be divided into three components: that required for making up heat losses (P_2), the useful input (P_u) and the input reserve, so that one can write

$$P = (P_u + P_2)\, k_r . \qquad (11)$$

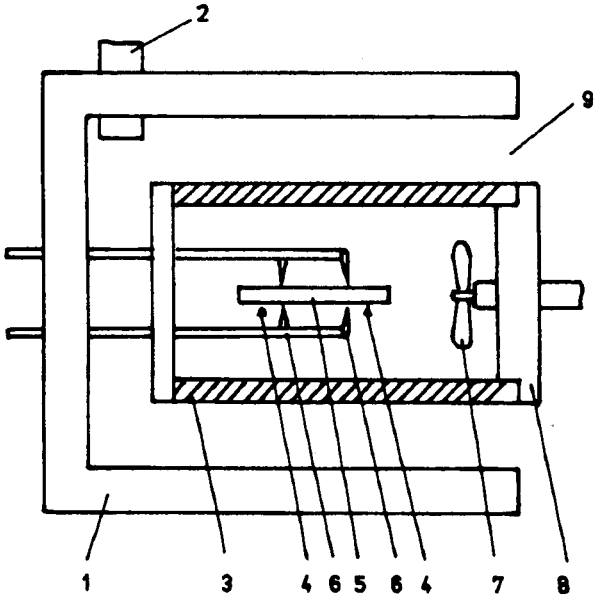

Fig. 1. Schematic diagram of the laboratory annealing kiln. 1 - outer thermal insulation (Sibral), 2 - cooling air supply tube, 3 - muffle with heating windings, 4 - corundum specimen supports, 5 - glass specimen, 6 - thermocouples, 7 - propeller, 8 - access opening lid, 9 - cooling air outlets.

Using procedures and equations described in the literature [16, 17, 18, 19], the total kiln input including the standby one was determined:

$$P = (0.095 + 0.54) \times 3 = 1.9 \text{ kW} \qquad (12)$$

The parameters of the heating kanthal wire were determined according to this input, using [20].

6.3 Measuring temperature in the kiln

The correctness of temperature control in the kiln depends to a considerable degree on the way the temperature is measured. Even if the temperature field is adequately homogeneous, the actual temperature course in the kiln need not be identical with the calculated annealing curve. To control the annealing process, one has to monitor continuously and with satisfactory accuracy the actual kiln temperature which must not show any deviations that would result in control delays.

Glass annealing is effected over the temperature range of 20 to 600°C, so that chromel-alumel thermocouples should be used. They are readily available, show a high EMF and its linear temperature dependence over the temperature interval in question. however, they have the disadvantage of requiring individual calibration owing to the variable quality of their arc-welded joints.

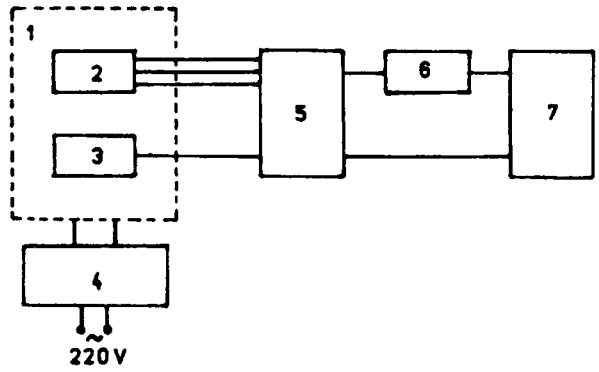

Fig. 2. Wiring diagram and temperature measurement during calibration of thermocouples (Chromel-Alumel). 1 - crucible furnace, 2 - chromel-alumel thermocouples, 3 - Pallaplat reference thermocouple, 4 - voltage controller (phase-type), 5 - analog multiplexer, 6 - A/D converter (MT 100), 7 - SAPI 1 computer.

A writing diagram and the way the temperature is measured during calibration, is illustrated in Fig. 2.

6.4 Design and installation of the measuring and control system

The complete system consists of three basic parts, namely

- the data acquisition subsystem,
- the data evaluating and control command subsystem,
- the action command subsystem.

A schematic diagram of the measuring and control system of the laboratory annealing kiln is given in Fig. 3.

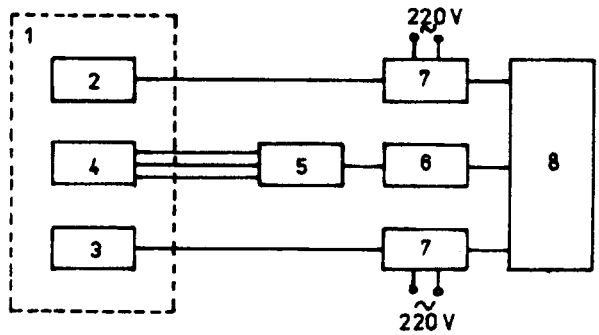

Fig. 3. Schematic diagram of the measuring and control system of the laboratory annealing kiln. 1 - annealing kiln, 2 - heating winding 1, 3 - heating winding 2, 4 - temperature measurement, 5 - analog multiplexer, 6 - A/D converter (MT 100), 7 - synchronous controller, 8 - SAPI 1 computer.

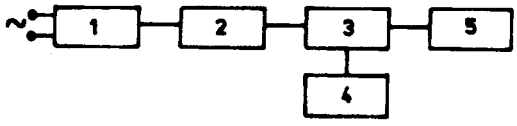

Fig. 4. Schematic diagram of the asynchronous power input controller of the laboratory annealing kiln. 1 – shaper, 2 – counter, 3 – comparator, 4 – SAPI 1 computer, 5 – power switching element.

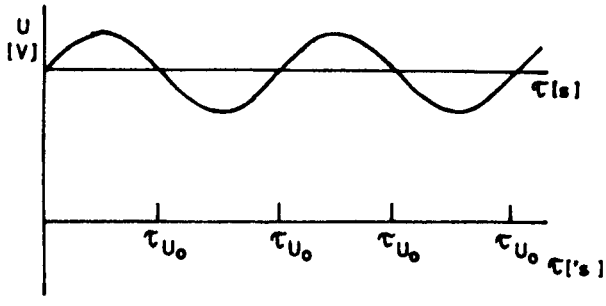

Fig. 5. Pulse generation by the forming circuit.

The data acquisition (kiln temperature) was implemented by measuring the EMF of the thermocouples connected via an eight-channel multiplexer to the MT 100 millivoltmeter and the SAPI 1 control computer, interconnected by a programmable parallel port board. The MT 100 served as a D/A converter.

The process data was evaluated and the control commands given by the SAPI 1 computer, for which the required software has been prepared.

The parallel transmission of action commands from the control computer to the synchronous controller was also effected through a parallel port board.

The actual kiln input controller was constructed according to the diagram in Fig. 4. The shaper generates pulses of mains frequency, with active edges occurring at the moment the mains voltage passes through its zero value, as shown by Fig. 5. With the arrival of each pulse from the shaper, the counter increases its state at output as a number ranging from O to 15. The comparator compares the counter with the value set by the computer and whenever the counter value is lower than the requested one, the comparator produces a control signal and the power contactor switches on the load. If the counter indicates a value higher than, or equal to, that required, the comparator transmits a passive control signal and the power contactor then turns off the load.

The kiln power was controlled by a thyristor supply source which has several advantages: a high switching frequency, high-precision control of electric quantities to constant values, instantaneous response to input signals, small size and great reliability. The value of the output electric quantity can be determined by phase or synchronous control. The principle of the two types of control is illustrated in Fig. 6.

Synchronous regulation was chosen for the measuring and control system, as it has the following advantages compared to phase regulation:

- It does not produce high-frequency interference on turning on the load, neither to the environment not to the power mains. Such interference could also affect the values of the thermocouple EMF being measured.
- It does not cause abrupt surges in the supply source load.
- It allows the electric quantities to be measured with current instruments as the quantities have a harmonic course, which is not the case of phase regulation.

To make the control of any arbitrary process by means of a measuring and control system based on computer technology precise, the measuring instrumentation has first to be perfectly experimentally described. In the case of annealing kilns, it is necessary to study in detail the responses of tempera-

Fig. 6. Schematic diagram of phase and synchronous regulation. 1 – phase regulation, 2 – synchronous regulation, 3 – active function of the regulator.

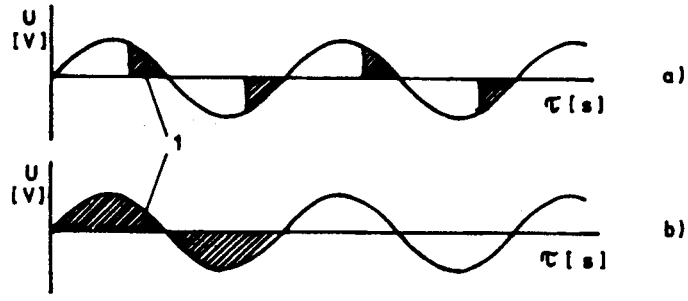

ture to jumping changes of power input, the so-called transition temperature characteristics. With annealing kilns, this should be done for both the heating up and cooling down stages. This represents measuring the time dependence of thermal properties of the kiln, and processing it into a form applicable in the computer control program.

The transition characteristics measured at various inputs are divided into several temperature intervals and their regression coefficients in equations (13 a, b) are determined by the least square method. For the heating-up stage,

$$t_i = A_{1p} + B_{1p}\tau_i \tag{13a}$$

For the cooling down stage,

$$t_j = D_{jp} + C_{jp}\tau_j \tag{13b}$$

For the control, it is of course necessary to determine relationship (14)

$$P = \mathrm{f}\left(\frac{\Delta t}{\Delta \tau}\right) \tag{14}$$

On the assumption that

$$\frac{\Delta t}{\Delta \tau} \doteq \frac{\mathrm{d}t}{\mathrm{d}\tau} \tag{15}$$

which is met with time dependence of temperature for both the heating up and cooling down stages, equations (14) and (15) yield equations (16 a, b) which are applicable for control purposes:
- for the heating up stage

$$\left[\frac{\Delta t}{\Delta \tau}\right]_i = B_{ip} \tag{16a}$$

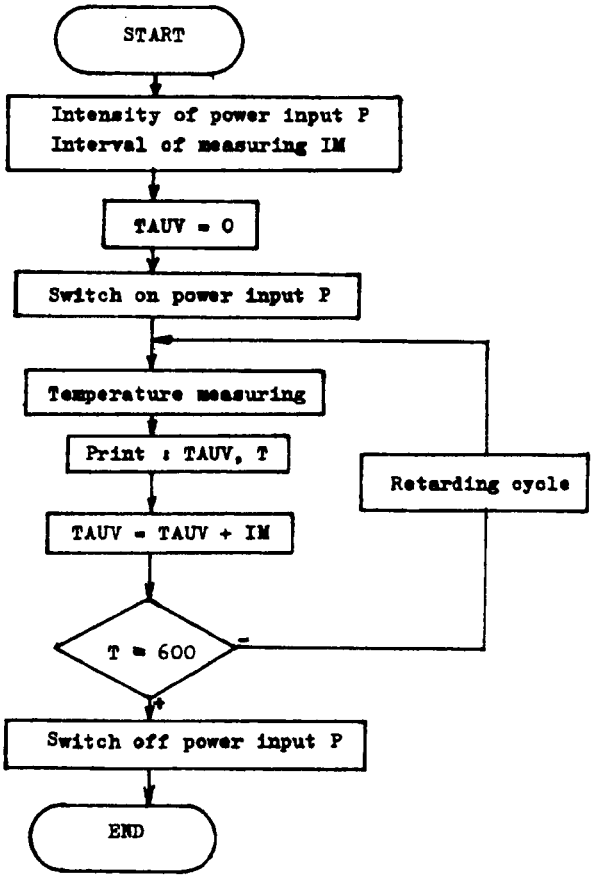

Fig. 7. Development diagram of the control program for measuring the transition characteristics for the heating range.

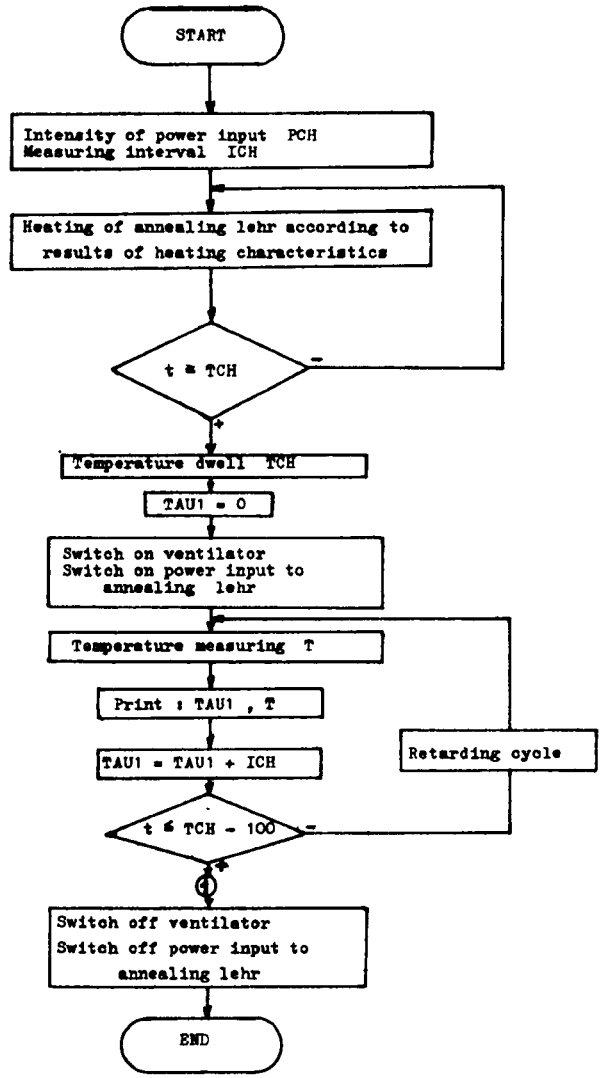

Fig. 8. Development diagram of the control program for measuring the transition characteristics for the cooling range.

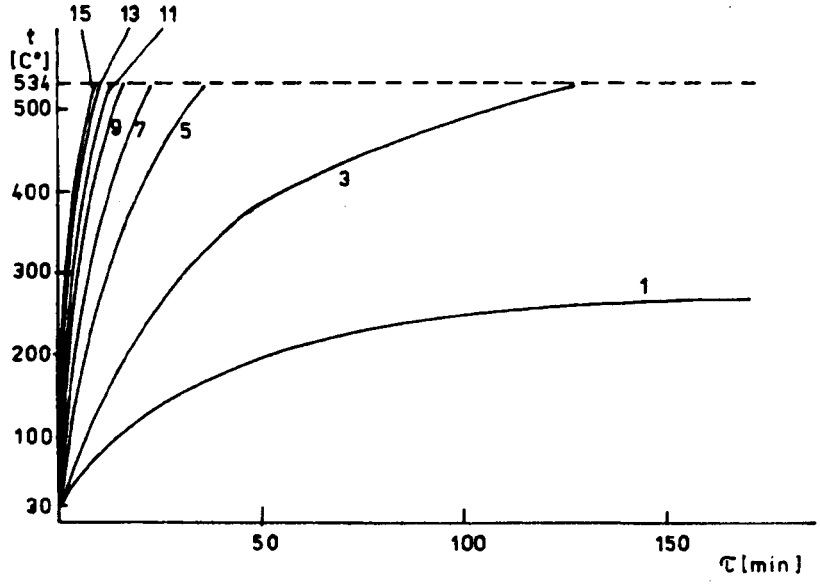

Fig. 9. Transition temperature characteristics for the heating range $P = (x/16)P_{max}$. *The values at the curves are those of quantity* x.

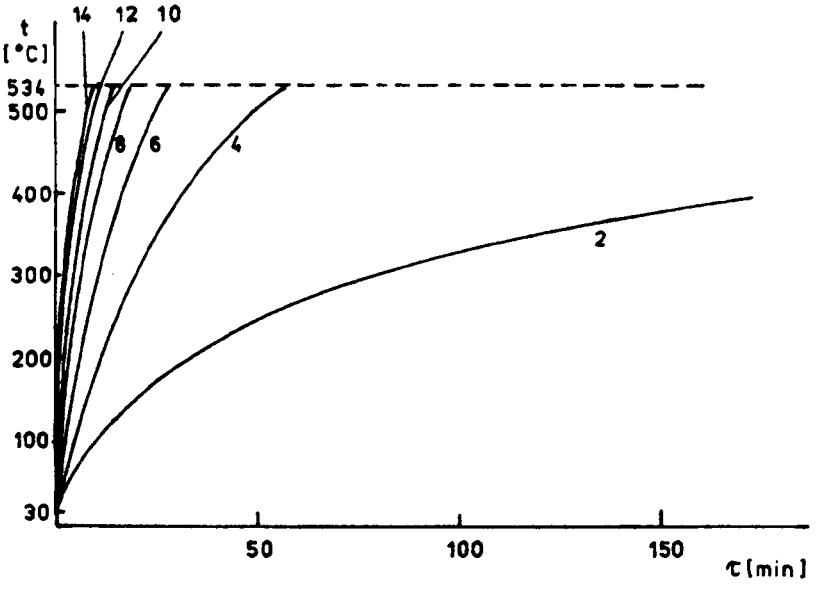

Fig. 10. Transition temperature characteristics for the heating range $P = (x/16)P_{max}$. *The values at the curves are those of quantity* x.

– for the cooling down stage

$$\left[\frac{\Delta t}{\Delta \tau}\right]_j = C_{jp} \tag{16b}$$

The temperature characteristics for the annealing kiln in question were measured by means of the computer-controlled measuring and control system. The structure of the control programs used in measuring the temperature characteristics is shown in the form of development diagrams in Figs. 7 and 8. The results of measuring the temperature characteristics are plotted in Figs. 9 and 10 for the heating up stage, and in Fig. 11 for the cooling down one.

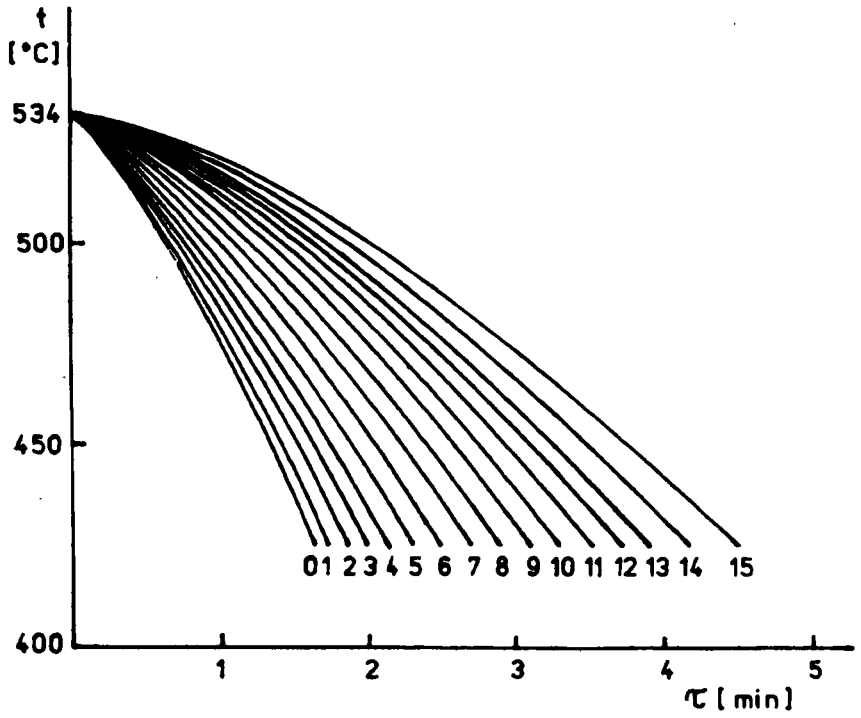

Fig. 11. Transition temperature characteristics for the cooling range $P = (x/16)P_{max}$. *The values at the curves are those of quantity* x.

7. EVALUATION OF THE RESULTS

The results were evaluated in two subsequent stages. First it was necessary to assess the transition temperature characteristics of the annealing lehr for the heating up and cooling down stages. Finally, the specific path differences were evaluated on specimens annealed in the kiln according a calculated annealing curve, and compared with the required specific path difference.

The transition temperature characteristics were evaluated by the procedure suggested in the previous chapter. The size of the temperature intervals were determined according to the curves shown in Figs. 9, 10 and 11, and from the intervals the values measured were approximated by linear regressive equations. The values of the calculated slopes of the temperature interval lines of the transition characteristics are listed in Table I for the range of heating up, and Table II for that of cooling down.

The control of power input into the annealing kiln and thus of its temperature was effected by means of a control program for the SAPI 1 computer, which is very suitable for these applications. The control procedure included a differentiation term and was based on comparing the required temperature (TZ) after a chosen control time (RD) with the temperature (T) measured at the given time. The difference between the two values determines the electric power supplied to the kiln at the moment of the next measurement. This again includes a comparison of the temperatures. The time of the regulation does not change, only its onset is delayed till the moment of this measurement. The value of the desired temperature is determined by the annealing curve whose overall course is not a linear function of time. The presence of the differentiation term in the control program allows the response of the system to the given intervention to be predicted. The value of the regulation time was chosen so as to be longer several times than the time intervals between the individual measurements, thus ensuring a smooth kiln temperature control, free from oscillation around the temperature required. A development diagram of the control program is shown in Fig. 12.

The specific path difference was measured on plate-shaped specimens by the polariscope using Sénarmont's compensator. The order of magnitude of the maximum path difference was established first, and only then the path difference determined quantitatively. The path difference is calculated from the equation

$$\bar{\Delta} = \frac{\lambda\Gamma}{180} \tag{17}$$

The path difference values were converted to specific

Table I

Slopes of transition characteristics for temperature in the heating up stage

$P = (X/16)P_{max}$	Temperature interval [°C]				
x[1]	100–200	200–300	300–400	400–500	500–540
1	2.8	0.1	–	–	–
2	7.0	4.1	0.7	–	–
3	10.8	7.7	4.2	1.5	0.1
4	14.0	10.8	7.2	3.8	1.8
5	18.3	14.8	11.4	7.6	5.3
6	22.5	19.0	15.5	11.7	9.0
7	26.7	23.3	19.6	15.8	12.7
8	29.9	26.8	22.6	18.9	15.4
9	33.1	30.1	26.0	22.4	18.5
10	35.9	33.3	30.0	27.5	23.5
11	39.1	36.7	33.5	32.0	29.0
12	43.3	40.9	39.0	36.6	33.1
13	46.5	44.2	42.7	41.1	38.3
14	50.8	48.5	47.0	45.6	43.5
15	55.0	52.8	51.2	49.8	48.4

Table II

Slopes of transition characteristics for temperature intervals in the cooling down stage

$P = (X/16)P_{max}$	Temperature interval [°C]						
x[1]	534–529	529–524	524–514	514–494	494–474	474–454	454–434
0	–50.0	–51.0	–52.0	–53.0	–54.0	–61.0	–60.0
1	–44.0	–48.0	–50.0	–50.5	–51.5	–58.5	–58.0
2	–41.5	–45.0	–48.0	–48.5	–50.0	–55.0	–56.0
3	–38.5	–43.0	–45.0	–45.5	–48.0	–52.0	–53.0
4	–36.0	–41.0	–42.0	–42.3	–47.0	–50.0	–50.0
5	–33.0	–39.0	–40.0	–40.5	–46.0	–49.0	–48.8
6	–31.0	–37.0	–38.0	–39.1	–45.0	–48.0	–45.0
7	–29.0	–35.0	–35.5	–38.1	–43.4	–47.0	–44.0
8	–27.0	–32.5	–33.0	–37.4	–41.4	–45.0	–42.6
9	–24.0	–30.0	–31.0	–36.3	–40.0	–43.0	–41.4
10	–20.0	–26.0	–29.5	–35.0	–38.0	–40.0	–40.0
11	–17.0	–22.0	–28.5	–33.6	–35.4	–37.7	–36.3
12	–14.0	–20.0	–27.0	–32.1	–34.0	–35.4	–35.0
13	–12.0	–18.5	–25.0	–31.1	–32.2	–32.9	–31.8
14	–10.0	–17.5	–22.0	–29.0	–30.0	–30.0	–28.2
15	–8.9	–16.5	–20.0	–26.8	–28.2	–27.0	–25.0

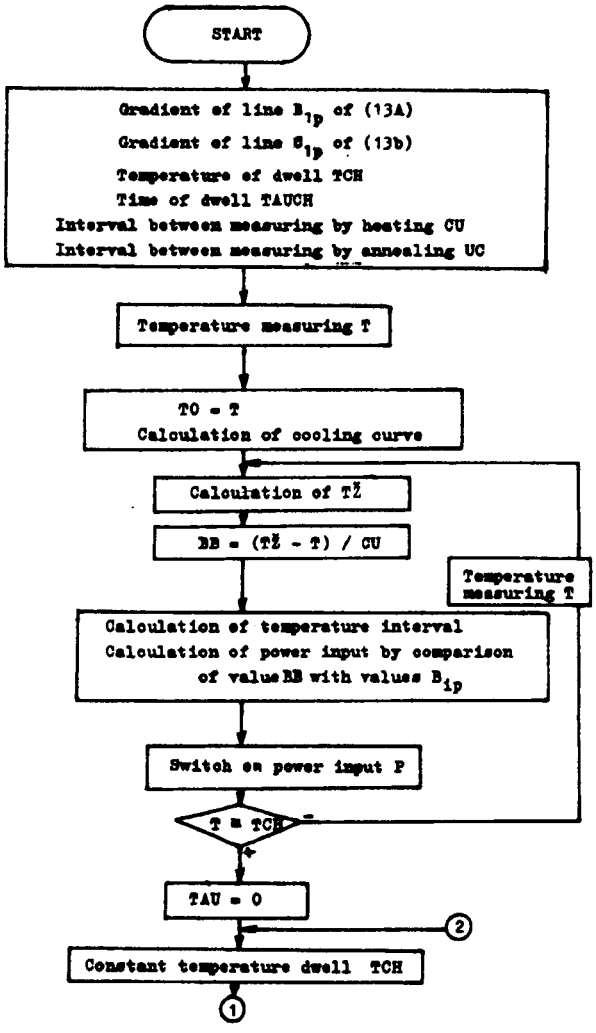

Fig. 12a. Development diagram of the control program for the annealing process.

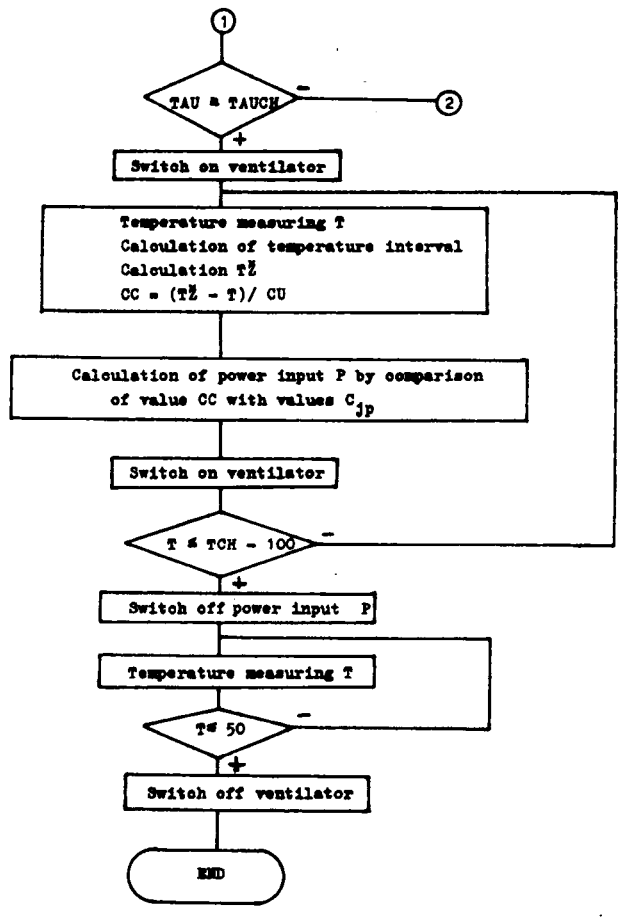

Fig. 12b. Development diagram of the control program for the annealing process.

path differences using the equation

$$x = \frac{\bar{\Delta}}{s} \tag{18}$$

The values of the compensation angles measured, the path differences and the specific path differences calculated are listed in Table III for the five specimens studied.

In the calculation of the annealing curve, the required specific path difference $X = 50$ nm.cm^{-1} was substituted into the equations. The results listed in Table III are in a very satisfactory agreement with the value substituted into the annealing curve calculation. This indicates that the actual controlled temperature course in the annealing kiln was in agreement with the calculated annealing curve, so that also the measuring and control system worked properly, together with the regulating system. The equipment has thus been proved suitable for annealing small-size sheet glass specimens and small glass ware of other shapes.

The measuring and control system is applicable for temperature and input control of all types of laboratory kilns and furnaces on the condition that the given kiln or furnace has first been experimentally described in detail. The procedures described in the experimental section of the present study may be used as operating instructions.

8. CONCLUSION

The present study had the aim to design and construct an annealing kiln whose temperature schedule would be computer-controlled by a control program, and to verify the validity of a calculated annealing curve in this kiln. The calculation of the annealing curve for plate glass specimens 10 × 10 × 0.5 cm yields very high values for the rates of heating, cooling and particularly final cooling, due to the small thickness and thus absence of any significant temperature gradients.

Table III

Maximum compensation angles measured, calculated path differences and specific path differences

Specimen No.	Γ [rad]	$\bar{\Gamma}$ [rad]	$\bar{\Delta}$ [nm]	X [nm cm^{-1}]
1	7.5 7.5 7.4	7.47	22.41	46.2
2	8.0 8.1 8.1	8.07	24.21	49.9
3	7.7 7.9 7.8	7.80	23.40	48.2
4	7.3 7.4 7.5	7.40	22.20	45.8
5	8.3 8.2 8.3	8.27	24.81	51.2

The high rates of temperature changes required during the annealing process made it necessary to create a kiln of non-traditional design, capable of meeting the requirements of the annealing curve while conforming to the demand for a temperature homogeneity of the kiln atmosphere. For this reason, the kiln was designed so as to allow for extensive outer cooling of the muffle by a fan, and for internal temperature homogenizing by means of a propeller. In this way it was possible to abide precisely by the temperature course given by the calculated annealing curve.

The annealing process, as one based on continuous heat transfer, is suitable for control by computer technology. Such a control system has been designed around the SAPI 1 computer, on the principle of utilizing the measured transition temperature characteristics of the annealing kiln. The computer control based on the software created is likewise advantageous, as it allows for arbitrary intervention into the control program, and thus for changing the annealing process. In this way it is possible to anneal specimens of other shapes, or to change the annealing schedule while maintaining the quality of glass required.

The above account indicates that the possibility of mastering the control of the annealing process is based on a suitable control program. The program described contained only a differentiation element which, in spite of its simplicity, has been proved satisfactory for controlling the annealing process under the conditions described in the present study. With an adequate number of experimental data, also another control element could be used, for example a PID controller. In such an instance, however, the problems involved would be qualitatively more complex and would require team cooperation with experts from the field of regulation and control.

Acknowledgement: The authors wish to thank Ing. S. Zrno, CSc for his valuable advice and assistence in the construction of the control system for the laboratory annealing kiln.

List of Symbols

a	thermal permittivity [m^2.s^{-1}]
E	Young's modules of elasticity [Pa]
h	heating rate [K.min^{-1}]
h_1	cooling rate [K.min^{-1}]
h_2	reserve coefficient [l]
K_1	constant (cf. (3))
N	coefficient (N=3 in (4))
P	output [W]
P_m	constant [Pa] (cf. (1))
s	plate half thickness [m]
t	temperature [C]
T	temperature [K]
x	distance from the surface [m]
X	specific path difference [nm.cm^{-1}]
α_D	coefficient of thermal expansion [K]
Γ	compensation angle [rad]
η	dynamic viscosity [Pa.s]
λ	dominant wavelength passed through filter [nm] (λ = 540 nm)
μ	Poisson's coefficient [l]
σ	stress [Pa]
τ	time [s]
τ_m	constant [s]
Θ	temperature gradient [K]
$\bar{\Delta}$	path difference [nm]

Subscripts:

max	maximum
0	initial
r	related to relaxation
x	related to layer x
u	useful
z	loss

References

[1] Schill F., Novotný V., Hrdina Z.: *Glass Annealing and Stress Control* (in Czech), SNTL Prague, 1968.

[2] Adams L. H., Williamson E. D.: Jour. Franklin Inst. *19*, 597, 835 (1920).

[3] Preston F. W.: Jour. Soc. Glass Technology *36*, 287 (1952).

[4] Ananic N. J.: Inform. techn. sbornik *5*, 60 (1957).
[5] Dauvalter N. J.: Stekol. promyshl. *11*, 28 (1939).
[6] Lillie H. R.: Jour. Amer. Cer. Soc. *16*, 619 (1933).
[7] Kavka J.: Inf. přehled SVÚS Hradec Král. *26*, No. 1 (1983).
[8] Indenbom V. L., Ananic N. J.: Steklo i ker. *15*, 11 (1958).
[9] Kasa S.: Glass Annealing (in Czech), KTS VŠCHT Praha'82
[10] Mazurin O. V., Lalykin N. V.: Fyz. i chimia stekla*6*, 622 (1980).
[11] Mazurin O. V., Lalykin N. V.: Steklo i ker. *42*, 13 (1984).
[12] Mazurin O. V., Lalykin N. V.: Steklo i ker. *43*, 7 (1985).
[13] Januskiewicz K. T.: Elektrowaerme intern. *39*, 326 (1981).
[14] Šašek et al.: Papers of VŠCHT Praha, series L7, 1977, p. 149.
[15] Schill F.: Research report, SVÚS Hradec Králové, 1970.
[16] Němeček M.: *Fundamentals of thermal calculations* (in Czech), ČVUT Praha, 1983.
[17] Mika V. et al.: *Collected calculation methods of chemical engineering* (in Czech), SNTL Praha, 1981.
[18] Pešek J.: *Thermally insulating materials and their applications* (in Czech), ČKZ Praha, 1984.
[19] Rada J.: *Electrothermal technology I* (in Czech), ČVUT Praha, 1985.
[20] Technical Guidebook, Kanthal Ltd., Hallstahamar, Sweden 1962.
[21] Novotný V.: Sklář a keramik *35*, 106 (1985).

PROCES CHLAZENÍ SKLA A JEHO ŘÍZENÍ

STANISLAV KASA, ANTONÍN LISÝ, ROMAN RANDÁK*

Ústav skla a keramiky, Vysoká škola chemicko-technologická, Technická 5, 166 28 Praha 6
**Sklárny Rapotín, 788 14 Rapotín*

Chlazení skla je řízené tepelné zpracování, jímž se odstraňují velká vnitřní napětí ve výrobcích ze skla nebo se zabraňuje jejich vzniku. Proces chlazení skla je procesem nestacionárního sdílení tepla a proto je vhodné pro jeho řízení využít výpočetní techniky s jejími výhodami. Dosavadní způsoby analogové regulace požadovaný průběh teplotního režimu v chladicí peci zajišťují obtížně a s velkými náklady.

Cílem předkládané práce bylo navrhnout a sestavit laboratorní chladicí pec, jejíž teplotní režim by bylo možné řídit výpočetní technikou s vytvořeným řídícím programem a také ověřit platnost výpočtem navržené chladicí křivky na základě porovnání napětí ve vzorcích skla Float ve tvaru destiček po vychlazení v řízené chladicí peci s požadovaným napětím ve vzorcích dosazovaným do výpočtu chladicí křivky.

Navržená laboratorní chladicí pec nové konstrukce umožňovala dodržet v peci požadovaný teplotní režim. Šlo zvláště o dodržení vysokých hodnot rychlostí vyhřívání a chlazení, což bylo dáno tvarem použitých vzorků, tj. malou jejich tloušťkou zabraňující vzniku výrazných teplotních gradientů ve vzorcích ve tvaru desky.

K dodržení vypočteného teplotního režimu v chladicí peci byl použit počítač (SAPI 1). Z tohoto důvodu byl také navržen měřicí a řídicí systém laboratorní chladicí pece, vycházející z předem proměřených přechodových teplotních charakteristik pece jak v oblasti vyhřívání, tak i v oblasti chlazení. Navržené a sestavené softwarové řízení se ukázalo jako velmi výhodné, neboť umožňuje libovolný zásah do řídícího programu a tím i změny v procesu chlazení.

Navržená laboratorní chladicí pec, stejně jako měřicí a řídicí systém byly hodnoceny pomocí naměřeného mechanického napětí ve vzorcích skla, které byly vychlazeny v chladicí peci řízené počítačem. Ukázala se velmi dobrá shoda mezi naměřeným mechanickým napětím ve vzorcích skla vychlazených v navržené laboratorní chladicí peci a požadovaným napětím sloužícím k výpočtu chladicí křivky.

Obr. 1. Schéma laboratorní chladicí pece: 1 – vnější izolace pece (Sibral), 2 – trubice pro přívod chladicího vzduchu, 3 – mufle s topným vinutím, 4 – korundové nosníky vzorku, 5 – chlazený vzorek skla, 6 – termočlánky, 7 – vrtule, 8 – víko vstupního otvoru mufle, 9 – otvory pro odvod chladicího vzduchu.

Obr. 2. Schéma zapojení a způsob měření teploty během kalibrace termočlánků (Chromel-Alumel). 1 – kelímková pec, 2 – termočlánky Chromel-Alumel, 3 – referenční termočlánek Pallaplat, 4 – regulátor napětí zdroje (fázový), 5 – analogový multiplexer, 6 – A/D převodník (MT 100), 7 – počítač SAPI 1.

Obr. 3. Schéma měřícího a řídícího systému laboratorní chladicí pece: 1 – chladicí pec, 2 – 1. topné vinutí, 3 – 2. topné vinutí, 4 – měření teploty, 5 – analogový multiplexer, 6 – A/D převodník (MT 100), 7 – synchronní regulátor, 8 – počítač SAPI 1.

Obr. 4. Schéma synchronního regulátoru příkonu do laboratorní chladicí pece: 1 – tvarovač, 2 – čítač, 3 – komparátor, 4 – počítač SAPI 1, 5 – výkonový spínací prvek.

Obr. 5. Generování impulsů tvarovačem.

Obr. 6. Principiální schéma fázové a synchronní regulace: a – fázová regulace, b – synchronní regulace, c – aktivní činnost regulátoru.

Obr. 7. Vývojový diagram řídícího programu pro měření přechodových charakteristik pro oblast vyhřívání.

Obr. 8. Vývojový diagram řídícího programu pro měření přechodových charakteristik pro oblast chlazení.

Obr. 9. Přechodové teplotní charakteristiky pro oblast vyhřívání $P = (x/16)P_{max}$. Hodnoty u křivek udávají veličinu x.

Obr. 10. Přechodové teplotní charakteristiky pro oblast vyhřívání $P = (x/16)P_{max}$. Hodnoty u křivek udávají veličinu x.

Obr. 11. Přechodové teplotní charakteristiky pro oblast chlazení $P = (x/16)P_{max}$. Hodnoty u křivek udávají veličinu x.

Obr. 12. Vývojový diagram řídícího programu chladicího procesu.